

NASA TECHNICAL
MEMORANDUM



NASA TM X-2629

NASA TM X-2629

AERODYNAMIC AND ACOUSTIC
PERFORMANCE OF TWO CHOKED-FLOW
INLETS UNDER STATIC CONDITIONS

by Brent A. Miller and John M. Abbott

Lewis Research Center

Cleveland, Ohio 44135

1. Report No. NASA TM X-2629	2. Government Accession No.	3. Recipient's Catalog No.	
4. Title and Subtitle AERODYNAMIC AND ACOUSTIC PERFORMANCE OF TWO CHOKED-FLOW INLETS UNDER STATIC CONDITIONS		5. Report Date September 1972	
		6. Performing Organization Code	
7. Author(s) Brent A. Miller and John M. Abbott		8. Performing Organization Report No. E-7008	
		10. Work Unit No. 741-72	
9. Performing Organization Name and Address Lewis Research Center National Aeronautics and Space Administration Cleveland, Ohio 44135		11. Contract or Grant No.	
		13. Type of Report and Period Covered Technical Memorandum	
12. Sponsoring Agency Name and Address National Aeronautics and Space Administration Washington, D.C. 20546		14. Sponsoring Agency Code	
15. Supplementary Notes			
16. Abstract <p>Tests were conducted to determine the aerodynamic and acoustic performance of two choking flow inlets under static conditions. One inlet choked the flow in the cowl throat by an axial translation of the inlet centerbody. The other inlet employed a translating grid of airfoils to choke the flow. Both inlets were sized to fit a 13.97 cm diameter fan with a design weight flow of 2.49 kg/sec. The inlets were operated in both the choked and unchoked modes over a range of weight flows. Measurements were made of inlet pressure recovery, flow distortion, surface static pressure distribution, and fan noise suppression. Choking of the translating centerbody inlet reduced blade passing frequency noise by 29 dB while yielding a total pressure recovery of 0.985. Noise reductions were also measured at 1/3-octave band center frequencies of 2500, 5000, and 20 000 cycles. The translating grid inlet gave a total pressure recovery of 0.968 when operating close to the choking weight flow. However, an intermittent high intensity noise source was encountered with this inlet that precluded an accurate measurement of inlet noise suppression.</p>			
17. Key Words (Suggested by Author(s)) Inlet design Acoustic suppression Sonic inlet Pressure recovery Choked inlet		18. Distribution Statement Unclassified - unlimited	
19. Security Classif. (of this report) Unclassified	20. Security Classif. (of this page) Unclassified	21. No. of Pages 24	22. Price* \$3.00

AERODYNAMIC AND ACOUSTIC PERFORMANCE OF TWO CHOKED-FLOW INLETS UNDER STATIC CONDITIONS

by Brent A. Miller and John M. Abbott

Lewis Research Center

SUMMARY

Tests were conducted to determine the aerodynamic and acoustic performance of two choking flow inlets under static conditions. One inlet choked the flow in the cowl throat by an axial translation of the inlet centerbody. The other inlet employed a translating grid of airfoils to choke the flow. Both inlets were sized to fit a 13.97-centimeter-diameter fan with a design weight flow of 2.49 kilograms per second. The inlets were operated in both the choked and unchoked modes over a range of weight flows. Measurements were made of inlet pressure recovery, flow distortion, surface static pressure distribution, and fan noise suppression.

Choking of the translating centerbody inlet reduced blade passing frequency noise by 29 decibels while yielding a total pressure recovery of 0.985. Noise reductions were also measured at 1/3-octave band center frequencies of 2500, 5000, and 20 000 cycles.

The translating grid inlet gave a total pressure recovery of 0.968 when operating close to the choking weight flow. However, an intermittent high intensity noise source was encountered with this inlet that precluded an accurate measurement of inlet noise suppression.

INTRODUCTION

Future commercial aircraft presently under study, such as the near-sonic transport, the advanced supersonic transport, and STOL aircraft, will all be required to meet stringent noise specifications. The primary source of aircraft noise is the engine, and current unsuppressed designs cannot meet the future noise goals. Experiments have shown that compressor and fan noise radiating from the engine inlet can be reduced by choking the flow with either inlet guide vanes or contracting cowl walls (refs. 1 and 2). However, the high inlet flow velocities involved, combined with the requirement for keeping the

inlet as short as possible, can lead to severe degradation in pressure recovery and generation of large flow distortions for some inlet designs. Further experiments are required to define favorable designs. The purpose of the present investigation was to measure the static performance of two types of choking inlets. The first inlet tested obtained choked flow by an axial translation of the spinner or centerbody. The second inlet employed a translating grid of airfoils to choke the flow. The inlets were sized to fit a 13.97-centimeter-diameter fan. Inlet pressure recovery, flow distortion, surface static pressure distributions, and acoustic performance are presented for the inlets operating in both the choked and unchoked mode. Inlet passage Mach number distribution was determined with a traversing static pressure probe.

SYMBOLS

D_{\max}	inlet total pressure distortion parameter, (maximum total pressure - minimum total pressure)/(average total pressure)
D_{\min}	inlet total pressure distortion parameter, (average total pressure - minimum total pressure)/(average total pressure)
D_{rms}	inlet total pressure distortion parameter, (standard deviation of total pressure)/(average total pressure)
D_{th}	cowl throat diameter, cm
L	cowl length, cm
M	inlet Mach number assuming one-dimensional potential flow
N	fan rotational speed, rpm
R_H	flow passage hub radius at rake measuring plane, cm
R_T	flow passage tip radius at rake measuring plane, cm
W	distance from rake measuring plane to fan rotor, cm
X	axial distance from cowl highlight, cm
θ	fan inlet corrected temperature, fan inlet temperature in K/(288.2 K)

APPARATUS AND PROCEDURE

Figure 1 shows a general layout of the test setup including a test inlet, an adapter section, a fan, an exhaust duct, and an exhaust noise muffler. Also shown is the location of microphones used to measure inlet noise. The tests were conducted using a single

stage (13.97 cm diameter) tip turbine driven fan as both a suction source and noise generator. The fan has 16 rotor blades resulting in a blade passing frequency of 9600 hertz at the fan design speed of 36 000 rpm. Design pressure ratio is 1.25 at a weight flow of 2.49 kilograms per second. Inlets were mounted to the fan by use of an adapter section containing the supports for the stationary centerbody as well as total pressure rakes used to measure inlet performance. No measurements were taken downstream of the fan.

Inlet Design

Translating centerbody inlet. - Figure 2(a) shows the translating centerbody inlet in the unchoked mode with the centerbody retracted. This configuration resembles a conventional inlet and would be the operating mode of this inlet at cruise where inlet choking for noise suppression is not required.

Figure 2(b) shows the computed Mach number distribution through the inlet assuming one-dimensional potential flow. Mach number is plotted as a fraction of the distance from the highlight to the rake measuring plane at the design weight flow of 2.49 kilograms per second. The throat Mach number is 0.60 with an 8.2-percent area increase through the diffuser resulting in a Mach number of 0.53 at the rake measuring plane. The effective conical half angle of the diffuser is 1.57° . Details of the cowl and spinner design are given on a following figure.

Figure 3(a) shows the translating centerbody inlet in the takeoff choked mode with the centerbody extended. Cowl throat area was reduced by 15.84 percent by using a cylindrical spacer to place the spinner in the cowl throat. The inlet was sized so that the choked weight flow remained constant at the unchoked value of 2.49 kilograms per second. The design Mach number at the rake measuring plane is 0.53 as before.

The computed one-dimensional potential flow Mach number distribution from the throat to the rake measuring plane is shown in figure 3(b). Mach 1 occurs at the cowl throat plane. The effective conical half angle of the diffuser is now 5.19° .

Details of the cowl and spinner design are given in figure 4. The external cowl has a NACA series one shape and was designed to have a drag rise Mach number of approximately 0.80. The cowl internal lip is a two-to-one ellipse. The contraction ratio (high-light area/throat area) is 1.30. The spinner is a NACA series one design with a length-to-diameter ratio of one.

Translating grid inlet. - The translating grid inlet is shown in figure 5. The cowl and spinner used with this inlet are the same ones used with the translating centerbody inlet. The grids are shown separated as they would be during cruise operation. The flow is not choked in this mode of operation as can be seen by looking at the computed local Mach numbers shown in figure 5(b). A maximum one-dimensional potential flow Mach number of 0.59 is indicated through the four downstream airfoils at the design

weight flow of 2.49 kilograms per second. Note that the Mach number through the three upstream airfoils is approximately the same, 0.58. The seven airfoils are of equal thickness and were uniformly spaced across the duct. Two side fairings or fillets were used to reduce losses near the duct wall.

The airfoil sections used have the NACA 65₂ - 015 basic thickness shape with a chord of 3.48 centimeters and a maximum thickness of 0.523 centimeter. The downstream airfoils are approximately 1.8 chord lengths ahead of the rake measuring plane.

To choke this inlet at takeoff, the four downstream airfoils are moved forward into the plane of the three stationary upstream airfoils. The flow area through the grid is reduced by 16.68 percent. This mode of operation is shown in figure 6. Figure 6(b) shows the one-dimensional potential flow Mach number distribution through the airfoil grid at the design weight flow of 2.49 kilograms per second. Mach 1 occurs at the airfoil maximum thickness plane. The airfoils are now approximately 2.6 chord lengths ahead of the rake measuring plane.

Instrumentation and Data Reduction

Test instrumentation gave measurements of inlet noise levels, inlet pressure recovery, steady-state total pressure distortion, surface static pressures, and inlet passage static pressures. The details of the instrumentation follow.

Rake measuring plane. - As shown in figure 7, eight radial rakes were located in the adapter section at the rake measuring plane. The rakes were spaced each 45° with six area weighted total pressure tubes on each rake. Seven static pressure taps were located on the outer wall of the flow passage between the total pressure rakes.

Inlet cowl. - The inlet cowl was instrumented to measure surface static pressures as shown in figure 8. Eleven static pressure taps were located in a row at one circumferential position. Five of these were located on the inlet lip between the highlight and the throat, the remaining six were located in the diffuser. An additional five static pressure tips, spaced every 60°, were located in the cowl throat.

Inlet probe. - The inlet static pressure probe shown in figure 9 was used to measure static pressure at various positions within the inlet. For the translating centerbody inlet, the probe was designed to extend axially within the inlet to the rake measuring plane. The probe could be placed at any radial position within the inlet.

Noise measurements. - Noise data were taken with four microphones placed in front of the inlet as was shown in figure 1. The microphones were closely grouped about the inlet centerline eight fan diameters ahead of the inlet. The test area was not acoustically calibrated. However, the sound pressure levels from the four microphones were selectively averaged to minimize any irregularities induced by the test area. The microphone outputs were recorded on magnetic tape and then processed with a 1/3-octave band

analyzer. The fan exhaust noise was suppressed to permit an examination of only the noise being transmitted through the inlet. The hard walls surrounding the test area approximated a reverberant chamber precluding any measurement of noise directionality.

Test Procedure

An initial calibration test was run with a bellmouth replacing the inlet cowl. The weight flow measured by the instrumentation at the rake measuring plane was then corrected to agree with the measured bellmouth weight flow. This correction was then applied at the appropriate fan speeds in all the data runs with the inlet cowl in place.

Data were first taken without the inlet probe in place. Corrected fan speed was increased from 28 000 to 37 000 rpm in increments of 1000 rpm. The inlet probe was then installed and data were taken over the same range of corrected fan speeds to determine the static pressure at various locations within the inlet passage. Inlet pressure recovery, distortion, and noise characteristics were not measured with the probe in place. The same procedure was repeated for each of the four inlet configurations.

RESULTS AND DISCUSSION

In the following discussion, inlet performance data are presented in terms of the surface Mach number computed from the static pressure measurements made in the cowl throat. This Mach number approaches a constant value as the choking weight flow is reached and serves to indicate when the inlet has reached a choked flow condition. An average throat Mach number computed from the measured weight flow is also shown. This Mach number becomes sensitive to small errors in measured weight flow as Mach 1 is approached. Therefore, it is not used as the primary correlating parameter. However, it is useful in indicating the general level of throat velocity.

Translating Centerbody Inlet

Shown in figure 10 is the measured relation between fan corrected speed and cowl throat surface Mach number. Data for the inlet operating in the unchoked mode with the centerbody retracted is shown by the circular symbols. This curve shows only subsonic Mach numbers and a smooth increase in surface Mach number (and hence weight flow) as fan speed is increased. The curve obtained for the inlet operating in the choked mode is given by the square symbols. It shows supersonic surface Mach numbers at the higher fan speeds and a distinct flattening out in the surface Mach number above a corrected fan speed of approximately 33 000 rpm. This indicates that the inlet weight flow is no longer

increasing and that a choked flow condition exists.

Several data points are labeled on this figure by the letters A to E. For convenience in comparing data, these same data points are labeled on the figures that follow.

The average throat Mach number and total pressure recovery of the translating centerbody inlet are shown as functions of cowl throat surface Mach number in figure 11. The average throat Mach number was computed from the weight flow measured with the instrumentation located at the rake measuring plane. As mentioned earlier, this Mach number is sensitive to small errors in measured weight flow. However, it serves to indicate the general level of flow velocity in the inlet throat.

While operating in the unchoked mode, the total pressure recovery is 0.997 to 0.998 at all values of cowl throat surface Mach number. In the choked mode, with the centerbody extended, pressure recovery decreases as inlet Mach number is increased. At point A, where the surface Mach number is 0.86, a pressure recovery of 0.994 was obtained. The average throat Mach number at this condition was computed to be 0.66. However, at point C, where the surface Mach number is 1.235, the recovery has fallen to 0.985. The computed average throat Mach number at point C is 0.82. As the surface Mach number is increased above 1.26, there is an abrupt drop in total pressure recovery as a result of overdriving the inlet.

The pressure recoveries shown in figure 11 were obtained from the six area weighted pressure tubes on each of the eight total pressure rakes. Slightly lower values of total pressure recovery would have been computed if boundary layer measurements had been included.

Inlet steady-state distortion is shown in figure 12. The distortion generated while operating in the unchoked mode, shown by the circular symbols, does not show any trend with increasing cowl throat surface Mach number. When operating in the choked mode, shown by the square symbols, a steady increase in distortion with increasing inlet Mach number was obtained. At point A, the values of the distortion parameters are $D_{\max} = 0.0593$, $D_{\min} = 0.0533$, and $D_{\text{rms}} = 0.0134$. At point C, the distortion parameters have increased to $D_{\max} = 0.0934$, $D_{\min} = 0.0786$, and $D_{\text{rms}} = 0.0274$. Beyond a surface Mach number of 1.26 there is an abrupt increase in distortion. This coincides with the reduction in pressure recovery shown in figure 11.

Shown in figure 13 is the static pressure distribution measured in the cowl from the highlight to the rake measuring plane. Data are shown for the inlet operating in the choked mode at weight flows corresponding to data points A to D. Data point E shows static pressure distribution for the inlet operating in the unchoked mode at the same weight flow as point C. The shape of the curves indicates that there has been no large scale flow separation downstream of the throat. However, data point C shows a relatively flat static pressure distribution in the throat region not seen on the other curves. This may be due to a local separated flow region confined to the area just downstream of the throat.

The midannular passage Mach number determined from the inlet static pressure probe is shown in figure 14 with the inlet in the choked mode. Mach number is plotted against axial position within the inlet for two values of cowl throat surface Mach number. At a surface Mach number of 1.15, corresponding to a data point located between points B and C, the inlet is not choked. The inlet is fully choked when the surface Mach number is 1.25, approximately point D. Note that in both cases the maximum midannular passage Mach number occurs downstream of the cowl throat plane.

The reduction in 1/3-octave band sound pressure level obtained by choking the inlet is shown in figure 15 as a function of cowl throat surface Mach number. Several 1/3-octave frequency bands are shown along with the band containing the fan blade passing frequency. The reduction in sound pressure level was obtained by subtracting the value measured with the inlet in the choked mode from the value obtained with the inlet in the unchoked mode. This subtraction was done with the fan operating at approximately the same corrected speed for both modes of operation.

The data in figure 15 show an increase in suppression as cowl throat surface Mach number is increased to 1.235 (point C). A further increase in Mach number reduced the suppression in all but the lowest frequency band. A suppression of 29 decibels was measured at point C in the 8000-hertz frequency band containing the blade passing frequency. As can be seen from figure 11, the average throat Mach number at point C is approximately 0.82.

Shown in figure 16 is the relation between sound pressure level suppression at the blade passing frequency and inlet total pressure recovery. (Fan rpm is increasing to the left.) A maximum noise suppression of 29 decibels was measured at point C where the pressure recovery is 0.985. Note that both pressure recovery and noise suppression are reduced in moving toward point D from point C. This shows that for this inlet design the best acoustical performance was obtained before the inlet was completely choked. In listening to the model, a low intensity warbling sound was detected over a narrow range of fan speeds. This sound appeared to occur only at inlet flow condition lying approximately between data points C and D. This sound was not detected at other operating conditions. The noise floor of the test installation, which is determined by the fan exhaust noise, is not known and may be hiding a larger reduction in fan noise than shown.

Translating Grid Inlet

The relation between fan corrected speed and cowl throat surface Mach number for this inlet is shown in figure 17. Note that the Mach number shown was computed at the cowl throat, not at the minimum area located within the airfoil grid. Operation in the unchoked mode with the grids separated is shown by the circular symbols. When in this

mode of operation, there is a steady increase in surface Mach number with increasing fan speed. This indicates that weight flow is also steadily increasing.

Movement of the four downstream airfoils forward into the plane of the three stationary upstream airfoils gives the operating characteristic shown by the square symbols. At fan speeds below 31 000 rpm, the operating lines for the choked and unchoked modes are parallel. However, when the fan speed is increased above 31 000 rpm, the operating line for the choked operating mode begins to level off. This indicates that the flow is beginning to choke through the airfoil grid.

Average grid Mach number and inlet total pressure recovery are shown in figure 18. Pressure recovery in the unchoked mode, shown by the circular symbols, decreases gradually with increasing surface Mach number. A pressure recovery of 0.985 was obtained at point F where the design inlet weight flow of 2.49 kilograms per second was measured.

Pressure recovery when in the choked operating mode is shown by the square symbols. Pressure recovery decreases with increasing surface Mach number from a maximum value of 0.983 to a minimum value of 0.968 when the inlet is nearly choked. The corresponding average grid throat Mach number ranges from 0.66 to 0.84.

Inlet total pressure distortion is shown in figure 19. Note that the distortion measured when operating in the unchoked mode equals or exceeds that obtained when in the choked mode. This somewhat surprising result may be due to the increased spacing obtained between the airfoil grid and the rake measuring plane when in the choked operating mode. In all cases, the measured distortion parameter was less than 0.09. This is approximately the same value measured with the centerbody inlet when operating at the same throat Mach number.

Difficulties attributed to possible airfoil flutter were experienced in attempting to measure the acoustical performance of this inlet. An intermittent high intensity noise source was encountered when the airfoil Mach number was increased beyond approximately 0.78. This noise precluded measurement of accurate noise suppression data with this inlet. A narrow band frequency analysis indicated that this noise was being generated in the frequency range between 500 and 4000 hertz. However, just prior to the onset of this noise, a reduction of 7 decibels was obtained at the blade passing frequency.

SUMMARY OF RESULTS

Aerodynamic and acoustic performance of two choking flow inlets was determined under static conditions. The first inlet obtained choked flow by an axial translation of the centerbody. The second inlet employed a translating grid of airfoils to choke the flow. The results may be summarized as follows:

1. In the unchoked mode, a total pressure recovery of 0.997 to 0.998 was obtained with the translating centerbody inlet at the design weight flow of 2.49 kilograms per second.

2. In the choked mode, the total pressure recovery of the translating centerbody inlet was 0.985 with a 29-decibel suppression in fan blade passing noise. The average throat Mach number at this condition was computed to be 0.82 with a maximum total pressure distortion of 0.0934.

3. In the unchoked mode, the total pressure recovery of the grid inlet was 0.985 at the design weight flow of 2.49 kilograms per second.

4. In the choked mode, the pressure recovery of the grid inlet was 0.968 at an average Mach number of 0.84. Total pressure distortions measured with the grid inlet choked and unchoked were less than 0.09.

5. An intermittent high intensity noise was encountered when the grid inlet was operated at an average throat Mach number above approximately 0.78. This precluded an accurate measurement of inlet noise suppression.

Lewis Research Center,
National Aeronautics and Space Administration,
Cleveland, Ohio, June 27, 1972,
741-72.

REFERENCES

1. Chestnutt, David: Noise Reduction by Means of Inlet-Guide-Vane Choking in an Axial-Flow Compressor. NASA TN D-4682, 1968.
2. Anon.: Study and Development of Turbofan Nacelle Modifications to Minimize Fan-Compressor Noise Radiation. Volume V - Sonic Inlet Development. NASA CR-1715, 1971.

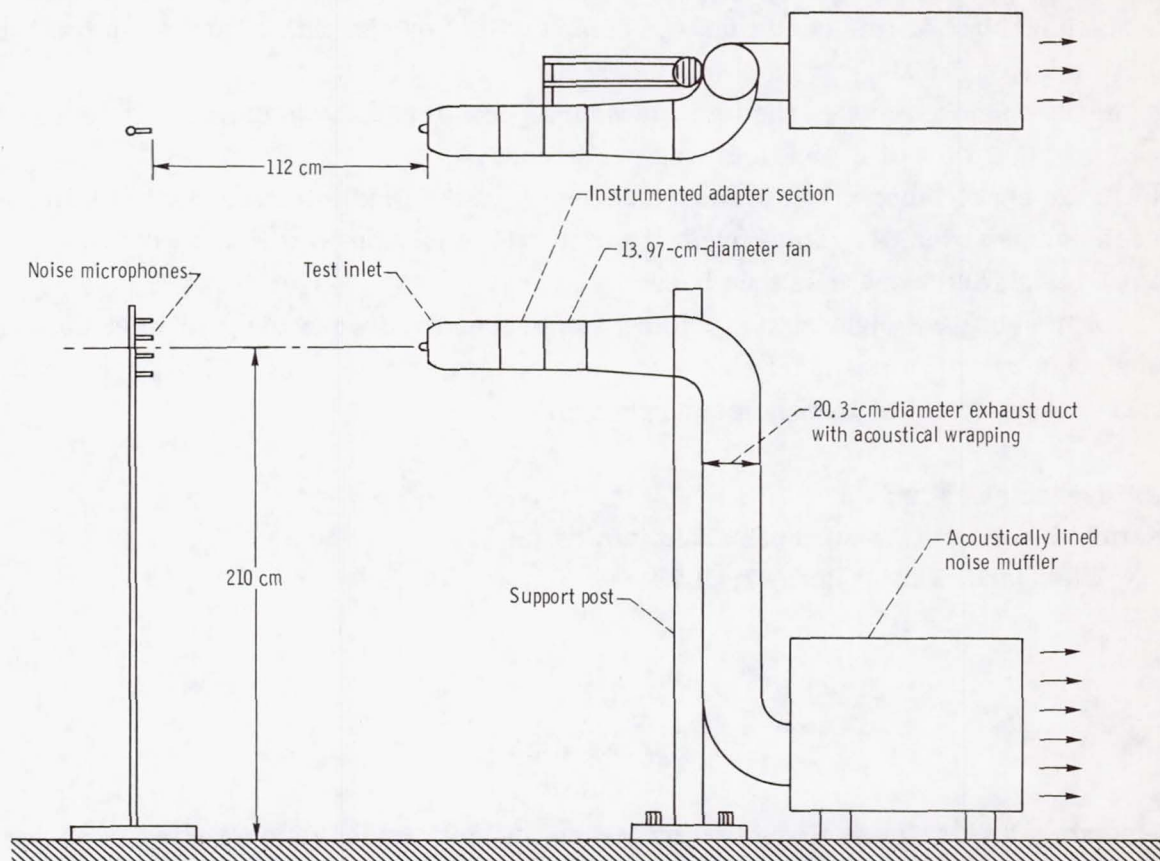
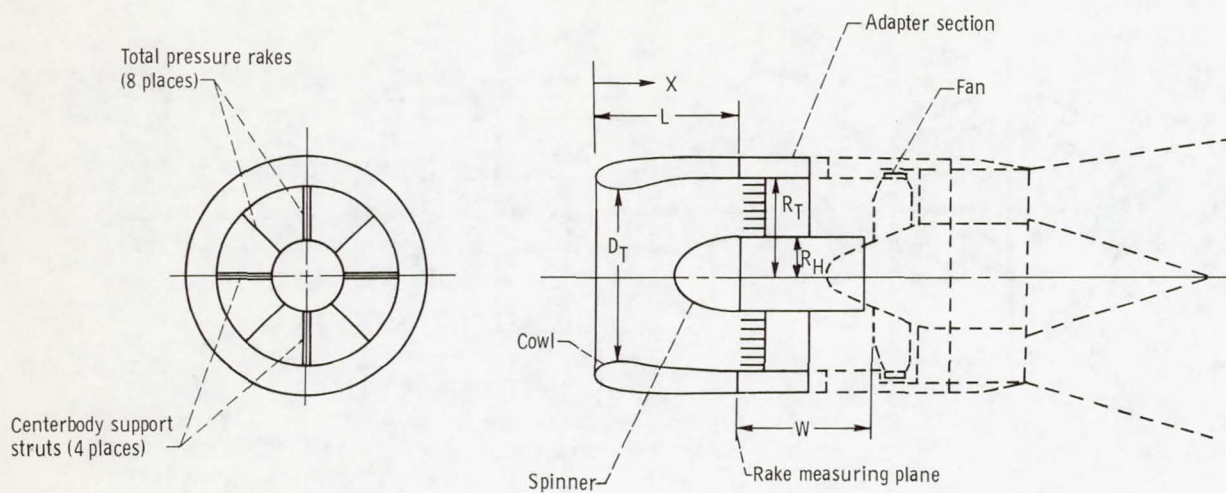
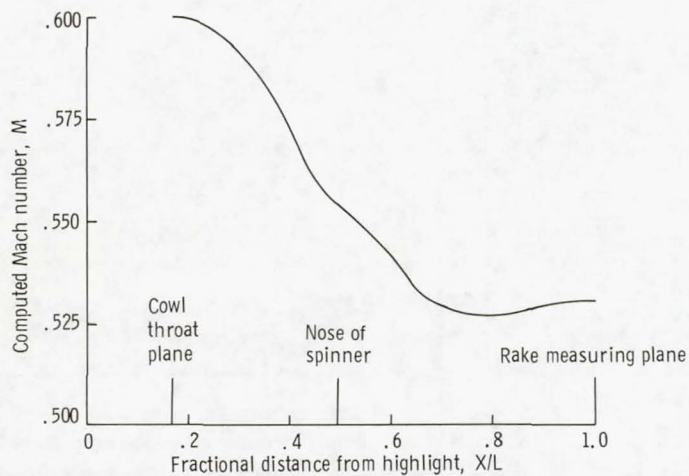


Figure 1. - Schematic layout of test rig.

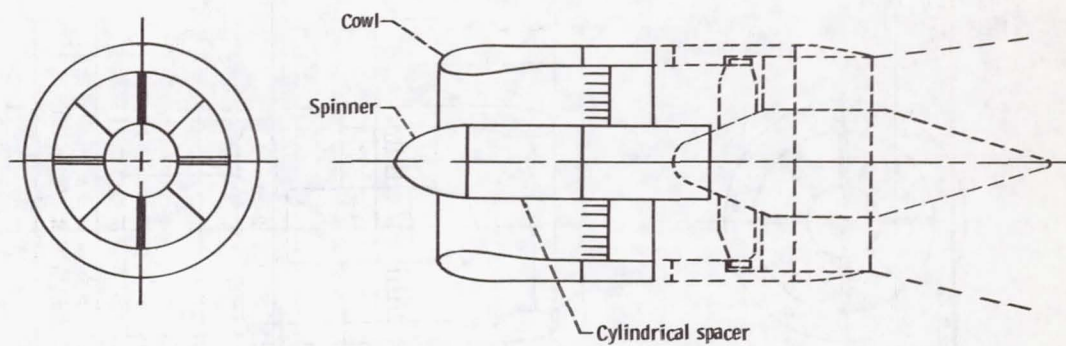


(a) Inlet schematic. Cowl throat diameter, D_T , 12.55 centimeters; cowl length, L , 10.24 centimeters; flow passage tip radius at rake measuring plane, R_T , 6.99 centimeters; flow passage hub to tip radius ratio, R_H/R_T , 0.364; and distance from rake measuring plane to fan rotor, W , 9.5 centimeters.

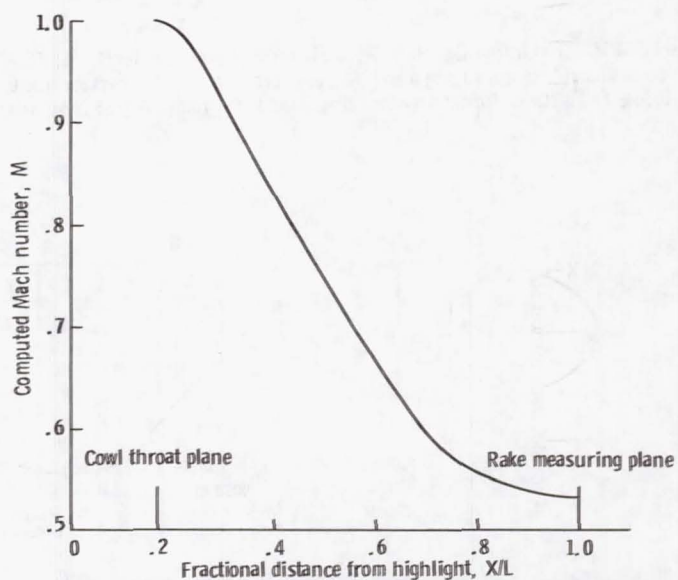


(b) Inlet Mach number distribution at design weight flow of 2.49 kilograms per second.

Figure 2. - Translating centerbody inlet in unchoked mode with centerbody retracted.

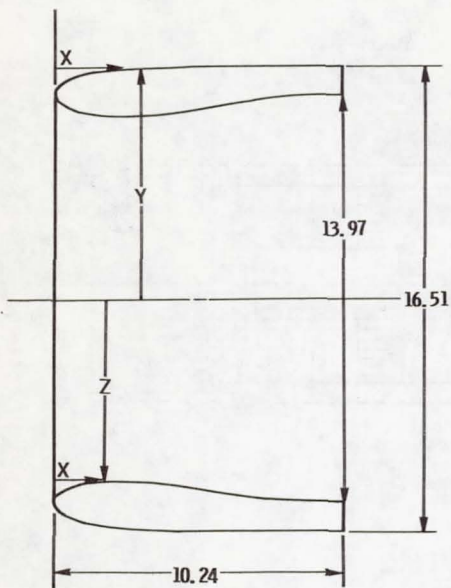


(a) Inlet schematic.



(b) Inlet Mach number distribution at design weight flow of 2.49 kilograms per second.

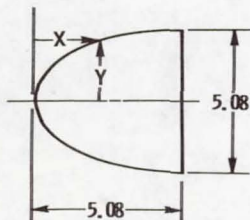
Figure 3. - Translating centerbody inlet in choking mode with centerbody extended.



X	Y
0	7.15
.02	7.23
.04	7.25
.10	7.32
.20	7.39
.40	7.50
.74	7.70
.99	7.73
1.24	7.81
1.49	7.87
1.98	7.98
2.48	8.06
2.97	8.20
3.47	8.21
3.96	8.22
4.46	8.25
4.95	8.26
.	.
.	.
.	.
10.24	↓

X	Z	X	Z
0	7.15	1.75	6.27
.05	6.94	1.98	6.28
.10	6.86	2.62	6.29
.15	6.79	3.25	6.30
.28	6.68	3.89	6.33
.41	6.59	4.52	6.38
.53	6.52	5.16	6.44
.66	6.47	5.79	6.55
.79	6.42	6.43	6.65
.91	6.38	7.06	6.75
1.04	6.35	7.70	6.85
1.17	6.32	8.33	6.91
1.30	6.30	8.97	6.95
1.42	6.29	9.60	6.98
1.57	6.28	10.24	6.99

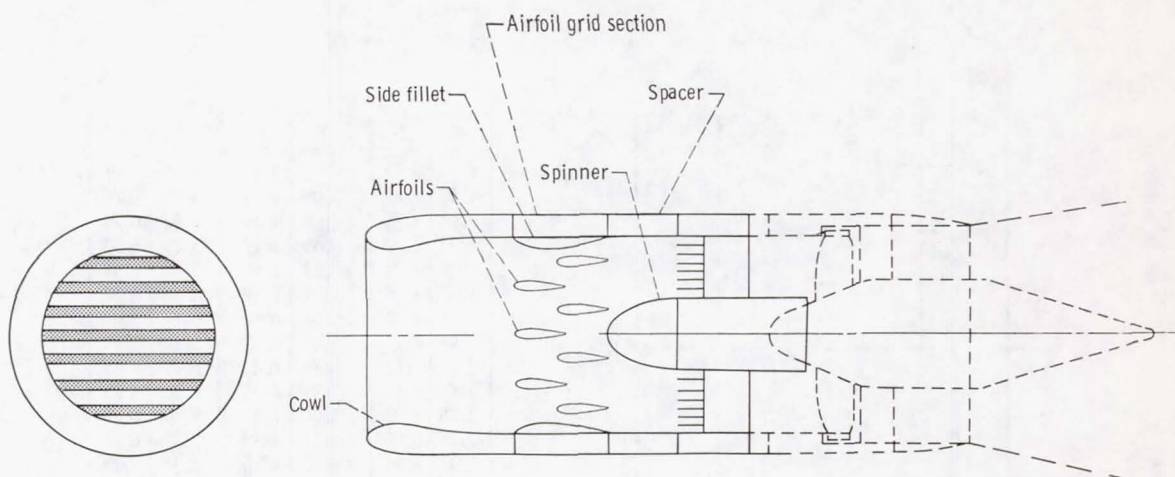
(a) Cowl.



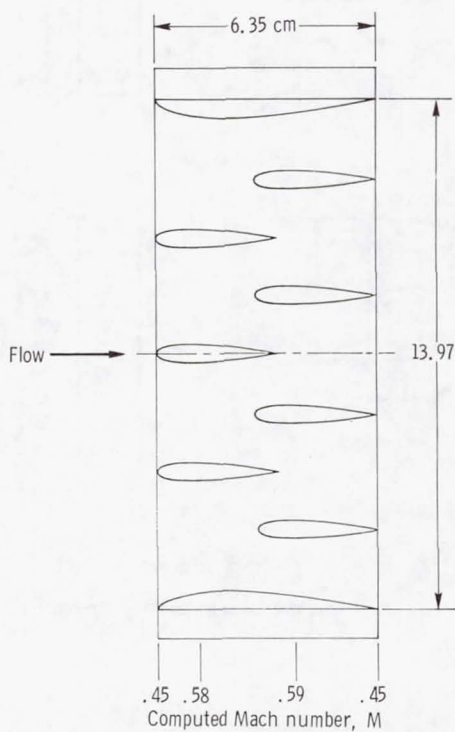
X	Y	X	Y
0	0	1.52	1.65
.10	.37	2.03	1.90
.20	.55	2.54	2.10
.30	.69	3.05	2.26
.41	.81	3.56	2.39
.51	.92	4.06	2.47
.76	1.15	4.57	2.52
1.02	1.34	5.08	2.54
1.27	1.50		

(b) Spinner.

Figure 4. - Details of cowl and spinner design. Dimensions are in centimeters.

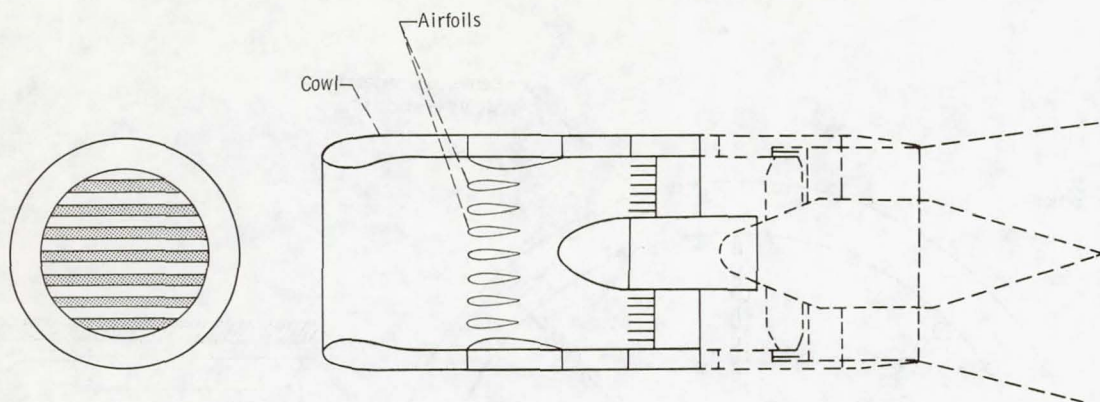


(a) Inlet schematic.

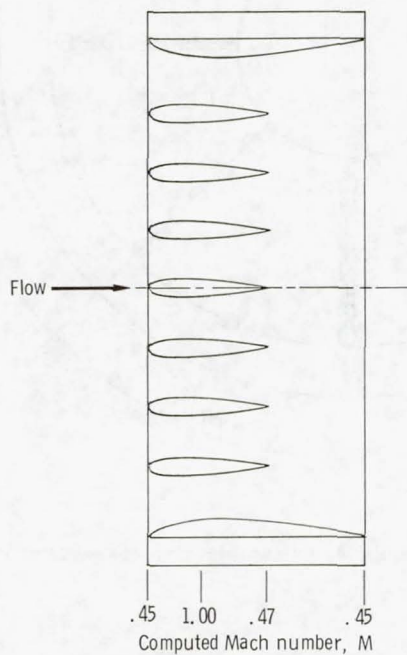


(b) Mach number distribution through airfoil grid at design weight flow of 2.49 kilograms per second. Airfoil thickness to chord ratio, 0.15.

Figure 5. - Translating grid inlet in unchoked mode with airfoil grids separated.



(a) Inlet schematic.



(b) Inlet Mach number distribution at design weight flow of 2.49 kilograms per second.

Figure 6. - Translating grid inlet in choked mode with downstream airfoils moved forward.

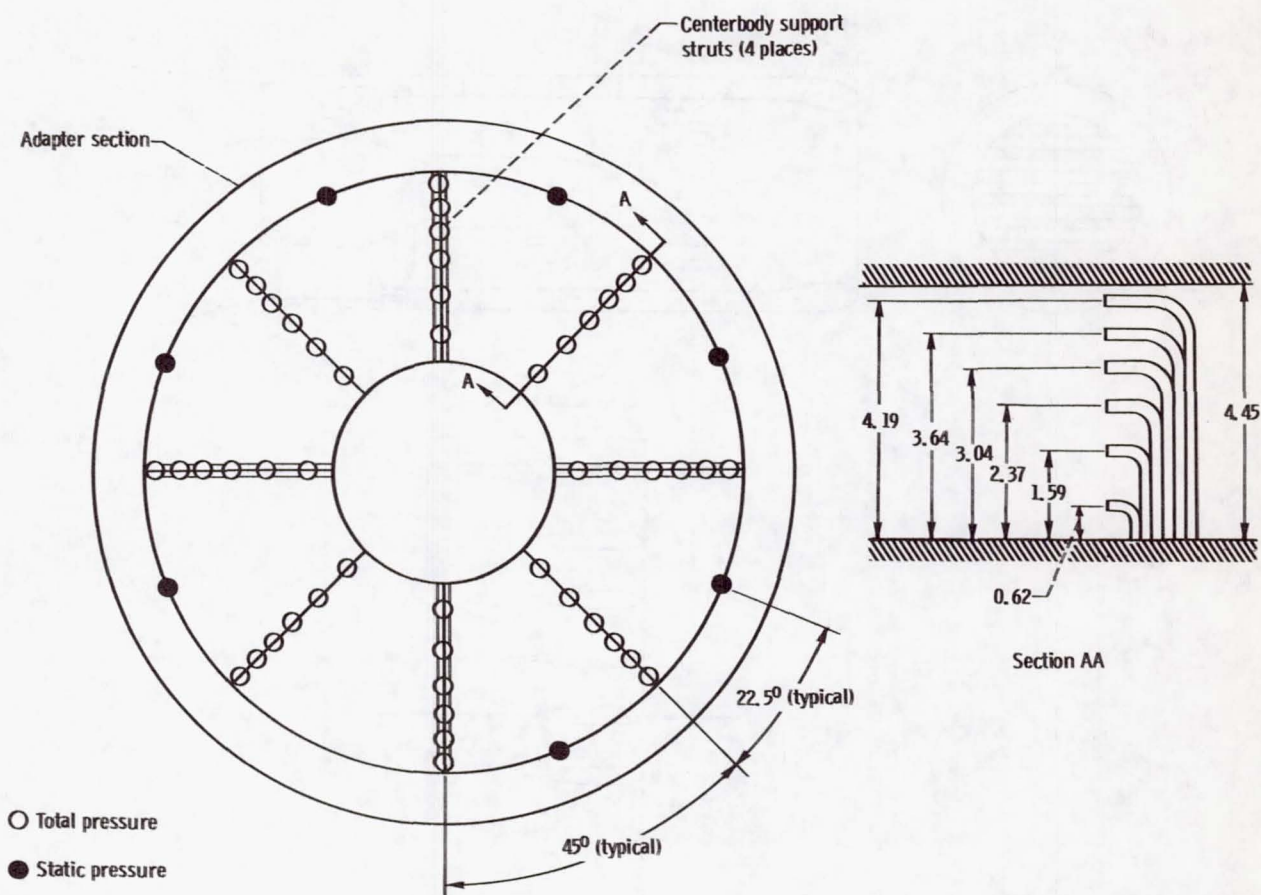
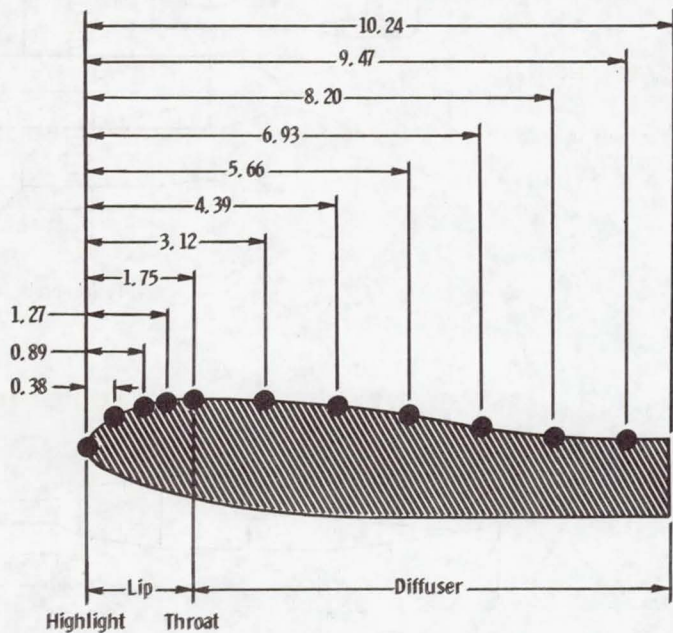
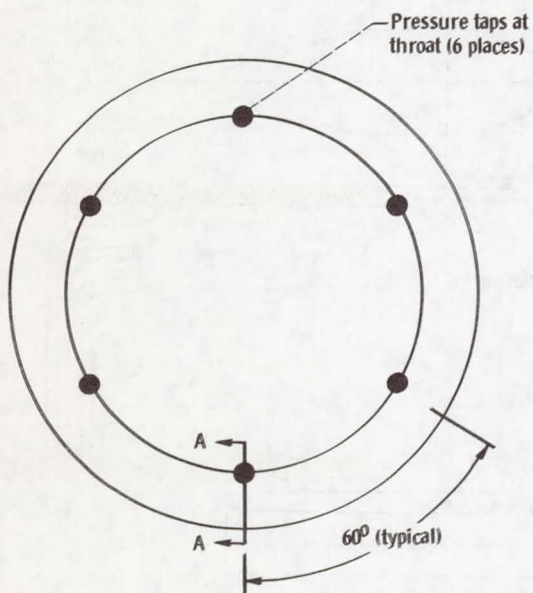


Figure 7. - Instrumentation schematic at rake measuring plane as viewed from upstream. Dimensions are in centimeters.

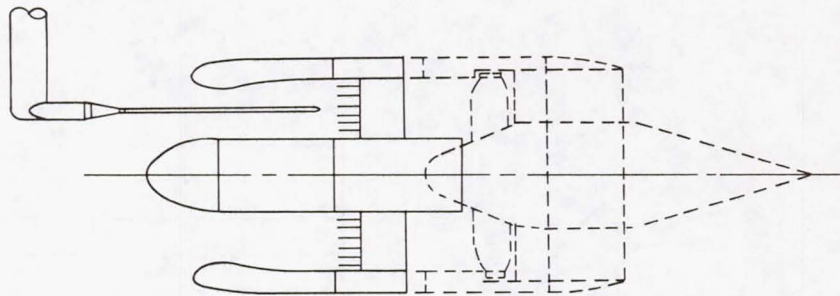


Section AA

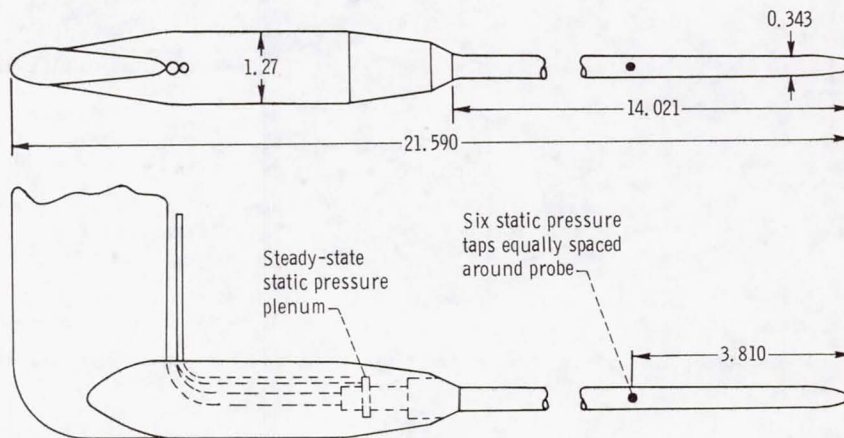
(a) Throat static pressure taps.

(b) Lip and diffuser static pressure taps.

Figure 8. - Instrumentation schematic for inlet cowl as viewed from upstream. Dimensions are in centimeters.



(a) Typical probe installation.



(b) Probe schematic.

Figure 9. - Inlet static pressure probe. Dimensions are in centimeters.

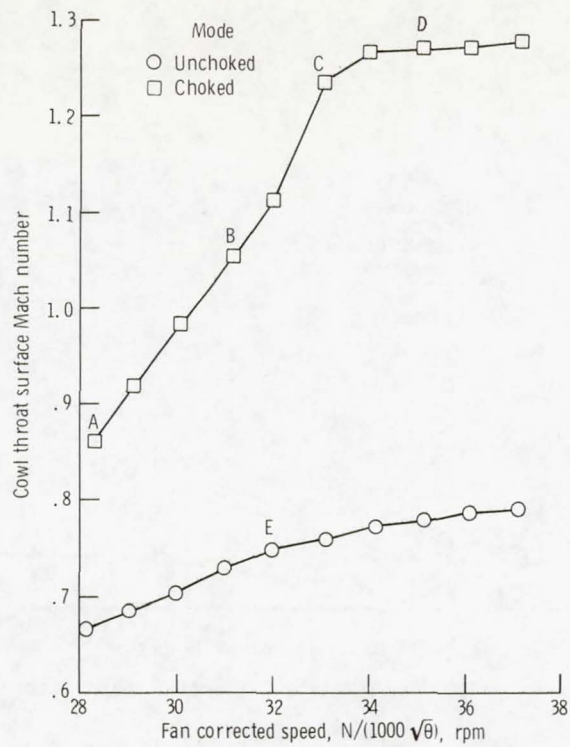


Figure 10. - Relation between cowl throat surface Mach number and fan speed for translating centerbody inlet.

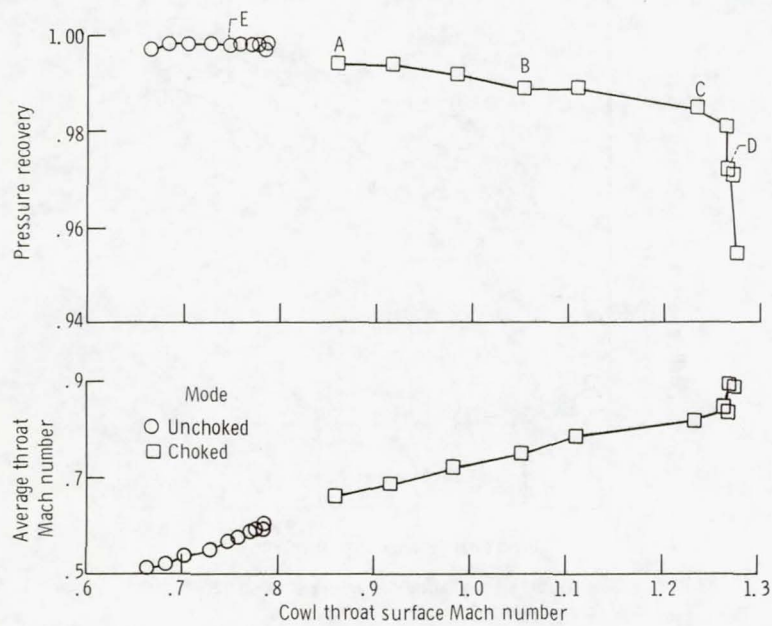


Figure 11. - Average throat Mach number and inlet pressure recovery of translating centerbody inlet.

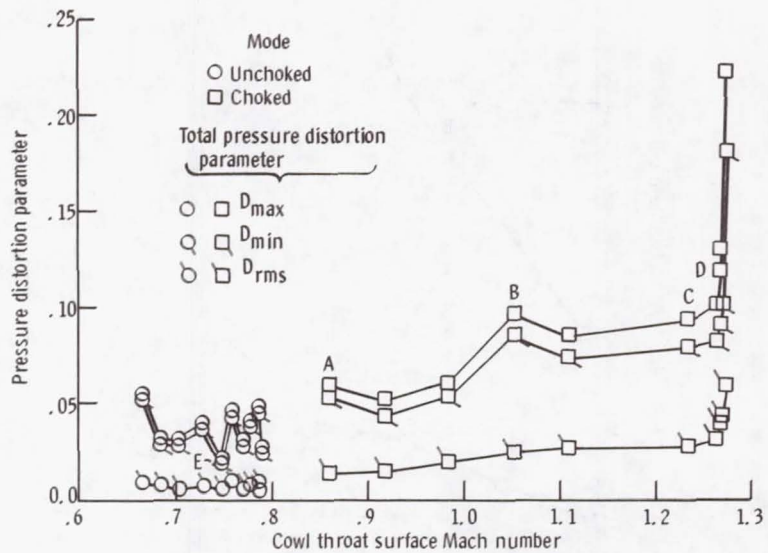


Figure 12. - Translating centerbody inlet total pressure distortion.

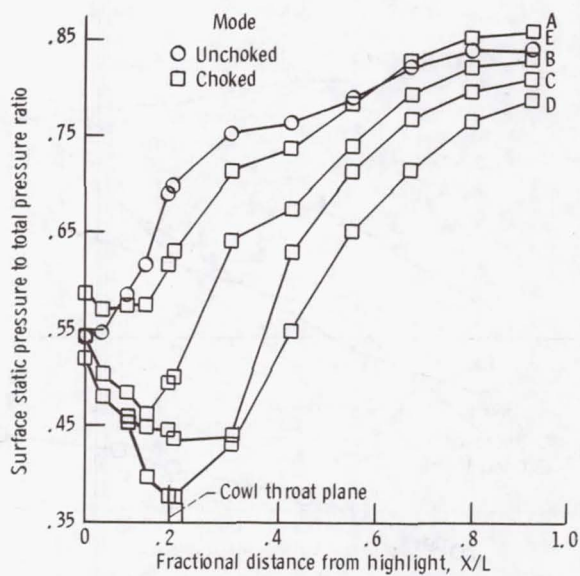


Figure 13. - Translating centerbody inlet surface static pressure distribution.

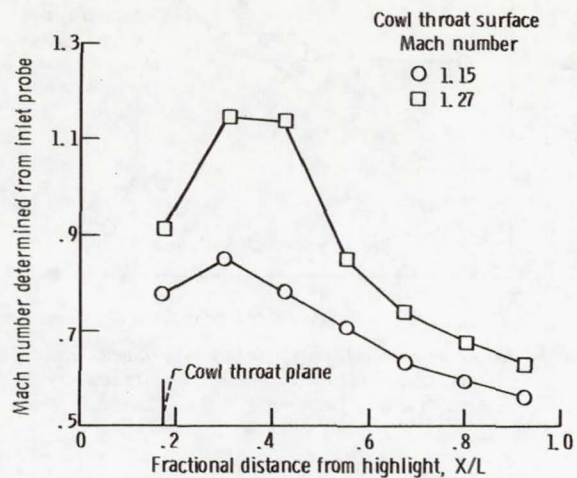


Figure 14. - Translating centerbody inlet Mach number distribution measured with inlet static pressure probe located 4.4 centimeters from inlet centerline. Inlet in choked mode.

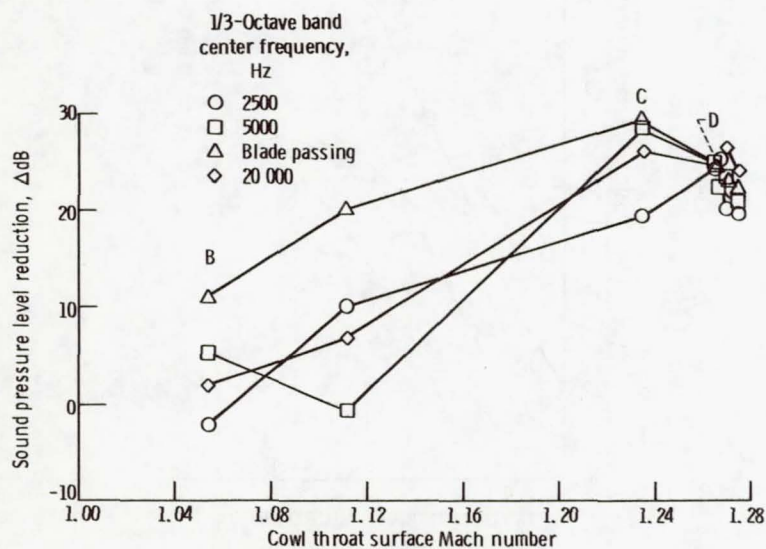


Figure 15. - Reduction in 1/3-octave band sound pressure level measured with translating centerbody inlet.

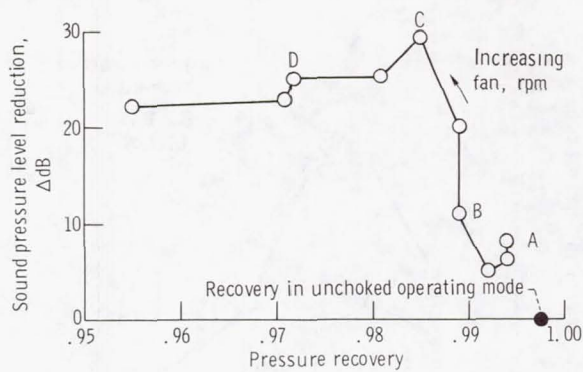


Figure 16. - Reduction in blade passing frequency sound pressure level as function of inlet pressure recovery. Translating centerbody inlet.

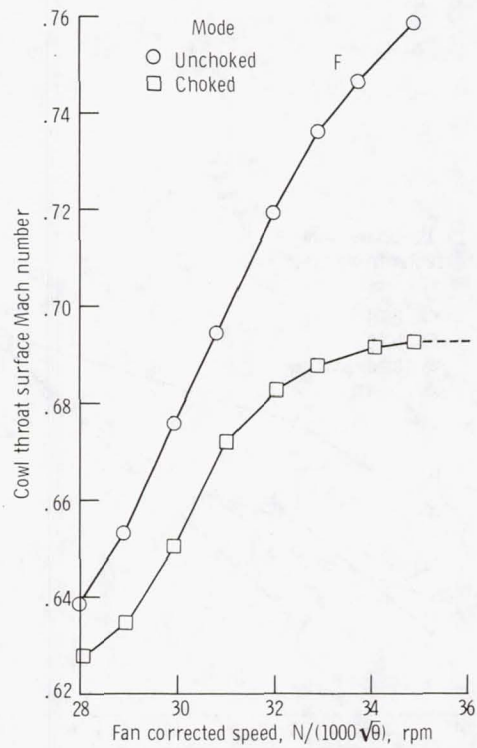


Figure 17. - Relation between cowl throat surface Mach number and fan speed for translating grid inlet.

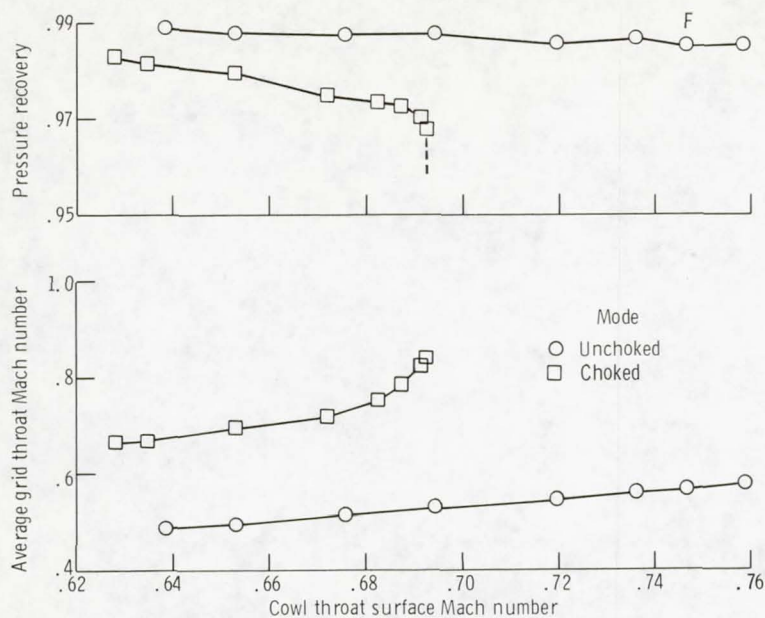


Figure 18. - Average grid throat Mach number and inlet pressure recovery of translating grid inlet.

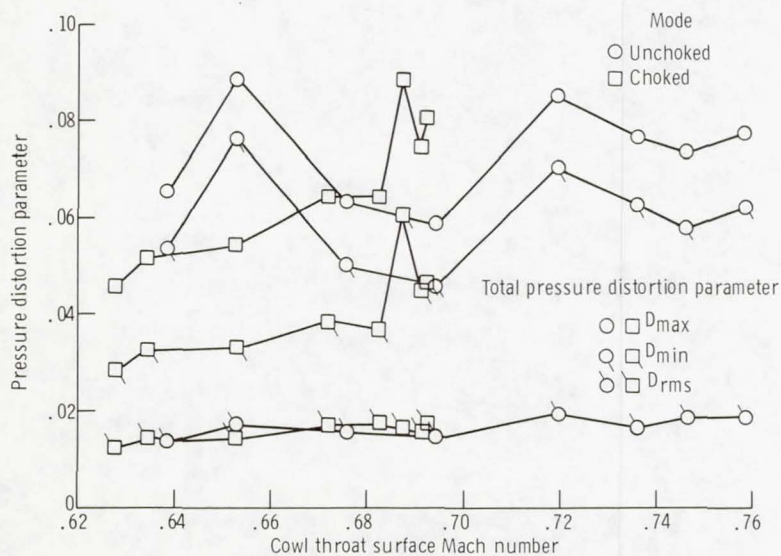


Figure 19. - Translating grid inlet total pressure distortion.